COLLOIDAL GOLD NANOPARTICLES: INTERACTION WITH OZONE AND ANALYTICAL POTENTIAL

Franco Cataldo[a,b]*, Ornella Ursini[c] and Giancarlo Angelini[c]

Keywords: gold nanoparticles; spherical particles; nanorods; ozone; ozone detection

Two different types of colloidal gold nanoparticles, produced as hydrosol, are recognized from their electronic absorption spectra. Gold nanorods with aspect ratio in the range between 2 and 4 and average diameter between 10 and 15 nm are produced using $AuCl_3$ and hydroxylamine. The surface plasmon resonance (SPR) band of gold nanorod undergoes a blue shift of about 50 nm on treatment with ozone. On the other hand, spherical gold nanoparticles with average diameter around 20 nm are produced from $AuCl_3$ reduced with black tea infusion. When treated with ozone the SPR band of the spherical gold nanoparticles show a red shift of more than 50 nm. This demonstrates that the shape of the gold nanoparticles deeply affects their response in the interaction with chemicals in view of the potential analytical application of gold nanoparticles as active materials in chemical sensors. A theoretical rationalization of the results is proposed.

* Corresponding Authors
E-Mail: franco.cataldo@fastwebnet.it
[a] Actinium Chemical Research,, Via Casilina 1626A, 00133 Rome, Italy
[b] Università della Tuscia, Dipartimento di Scienze Ambientali,Viterbo and Civitavecchia, Italy
[c] CNR–Istituto di Metodologie Chimiche, Area della Ricerca di Montelibretti, Via Salaria Km 29,300, 00016, Monterotondo, Scalo, Rome, Italy

Introduction

The formation and stability of silver nanoparticles was studied with the aid of "green" reagents, intended as reducing agents from renewable sources.[1,2] Tannin is found as an effective reducing agent of Ag^+ ion in the formation and stabilization of colloidal silver nanoparticles.[1] Similarly, the black and green tea infusions are effective agents in the formation and stabilization of colloidal silver nanoparticles.[2] The effectiveness of black and green tea infusions as reducing agents is essentially attributed to the polyphenols and other components present in the tea infusions.[2] Another "green" reducing agent suitable for the preparation of silver nanoparticles is the infusion of *Hibiscus Sabdariffa*, commonly known as "karkadé".[3] The karkadé infusions contain a series of anthocyanins and other components which have a reducing power comparable to that of tea polyphenols.[3] Using karkadé infusions it was possible to prepare silver nanoparticles in alkaline solutions by chemical reduction or in neutral-acidic solutions by radiation-induced nucleation reactions.[3] The importance of the studies on "green" reducing and capping agents for the synthesis of metal nanoparticles is testified by the numerous reviews.[4-11] Unexpectedly, certain synthetic agents are found as effective as tannin, polyphenols and anthocyanins in the synthesis of colloidal silver nanoparticles.[12-15] Heavily ozonized C_{60} fullerene,[12,13] as well as heavily ozonized C_{70} fullerene,[14] and ozonized single wall carbon nanohorns (SWCNH)[15] are also as effective agents in the formation and stabilization of colloidal silver nanoparticles.

The synthesis of gold nanoparticles is slightly less easier than the silver nanoparticles. However, a number of different synthetic methods are reported in some reviews.[16-19] The shape of the gold nanoparticles can be controlled with a high degree of confidence using tailor-made synthetic approaches.[19-24] The resulting surface plasmon resonance (SPR) electronic transition, typical of the gold nanoparticles, is deeply linked to the shape and size of the resulting gold nanoparticles.[23,24]

The interest in gold nanoparticles goes far beyond their antiseptic properties which is far surpassed by the silver nanoparticles.[2,25-31] In fact, gold nanoparticles find consolidated application as staining medium of tissues and cells in biology and biochemistry microscopy,[18,19] as well as effective antiarthritic agents.[32,33] Emerging potential applications of gold nanoparticles regard their quite easy surface functionalization and their use as drugs vector in general and in cancer therapy in particular.[34,35] Gold nanoparticles are also proposed as contrast agent to enhance the X-ray absorption on cancerous tissues or to enhance heating of tumor tissues in radio-frequency therapy.[34,35] The anti-angiogenic properties of gold nanoparticles can be employed to inhibit the vascularization of tumor masses.[34,35] Antiviral properties of functionalized gold nanoparticles were proved on laboratory scale and show great promise for larger scale applications.[35,36,37] However, safety and toxicological properties of gold nanoparticles in humans and in the environment are object of careful reviews.[38] Other fascinating applications of gold nanoparticles regard their use as active materials for chemical and biochemical sensors taking advantage of their optical and electrochemical properties.[19,23,39]

The present paper is related to the specific use of gold colloid hydrosols as sensitive material for the detection of ozone, and highlights the finding that the shape of gold nanoparticles in the form of nanorods or nanospheres give a completely different response in the interaction with ozone, a key know-how for future analytical applications.

Experimental

Materials and Equipment

$AuCl_3•3H_2O$ (Sigma-Aldrich) hydroxylamine hydrochloride (puriss, Fluka) and black tea bags were common commercial samples.
The electronic absorption spectra is studied using a Shimadzu UV2450 spectrophotometer using quartz cuvettes at 20 °C. The reference cuvette is filled with distilled water. Ozone was produced by corona discharge in dry air or oxygen at a rate of 400 mg h^{-1}.

Reduction of $AuCl_3•3H_2O$ with hydroxylamine

$AuCl_3•3H_2O$ (7.6 mg) was dissolved in 100 ml of distilled water. $NH_2OH•HCl$ (76.3 mg) was added to the gold solution, and the mixture stirred. The reduction reaction was followed spectrophotometrically monitoring the $AuCl_3$ absorption band at 310 nm. Although there was a disappearance of the band, no evidence for the formation of gold nanoparticles were detected.

Reduction of $AuCl_3•3H_2O$ with hydroxylamine at higher dilutions

$AuCl_3•3H_2O$ (6 mg) was dissolved in 500 ml of distilled water. $NH_2OH•HCl$ (25 mg) was added to the solution and quickly dissolved. The formation of colloidal gold was immediately observed because the solution turned into a beautiful blue colour. The reduction reaction was followed spectrophotometrically monitoring the colloidal gold surface plasmon resonance band at about 630 nm. Further additions of $AuCl_3•3H_2O$ in portions of 5-6 mg each caused a growth in the intensity of the SPR band and the solution changed its color from blue to blue-red although in transparency the solution appeared still deep blue.

Ozone treatment of blue gold hydrosol obtained with hydroxylamine

Blue colloidal gold solution (350 ml), prepared with hydroxylamine reduction as detailed in the previous section, having a nominal gold concentration of 20 mg L^{-1} was transferred in a Drechsell bottle and a mixture of ozone and air was bubbled in the hydrosol. Ozone was produced at a nominal rate of 400 mg h^{-1}. A series of spectra were taken after opportune intervals of time.

Reduction of $AuCl_3•3H_2O$ with black tea infusion

Black tea bag (2.0 g) was used to prepare an infusion in 150 ml of hot water for 2 min. Then, 50 ml of the infusion was diluted to a final volume of 450 ml with distilled water. $AuCl_3•3H_2O$ (6 mg) was dissolved in the diluted black tea infusion.

The reduction of Au^{3+} started immediately, was followed spectrophotometrically and confirmed by the development of the SPR band. The addition of further $AuCl_3•3H_2O$ in portions of 5-6 mg each caused a further increase in the intensity of the SPR band. The resulting solution had a magnificent dark-red color and is stable for months.

Ozone treatment of dark-red gold hydrosol obtained with black tea infusion

The dark-red coloured gold hydrosol (250 ml with a nominal gold content of about 22 mg L^{-1}), prepared as above, was transferred in a Drechsell bottle and a stream of ozone and air was bubbled in the hydrosol. Periodically samples of the solution were taken to record the electronic absorption spectra and to follow the interaction between ozone and the gold particles.

Results and Discussion

Reduction of $AuCl_3•3H_2O$ with hydroxylamine

The reduction of $AuCl_3$ into colloidal gold is not as easy as the reduction of silver into colloidal silver nanoparticles.

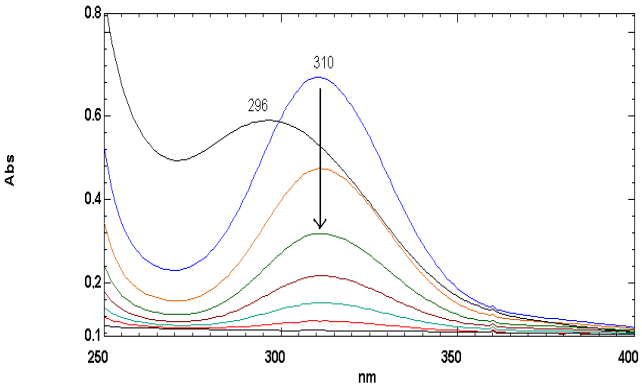

Figure 1. Electronic absorption spectra showing the reduction of the 310 nm absorption band of $AuCl_3$ by the action of hydroxylamine without the formation of colloidal Au.

Fig. 1 shows the absorption spectrum of a solution of $AuCl_3•3H_2O$ (7.6 mg/100 ml) with an absorption maximum at 296 nm which is shifted to 310 nm as soon as the reducing agent $NH_2OH•HCl$ is added. The absorption band at 310 nm which is due to the $AuCl_4^-$ anion,[40] started to decrease in intensity as function of time following pseudo-first order kinetics law as shown in Fig. 2 with a rate constant of $2.2x10^{-3}$ s^{-1}, and is in agreement with published results.[41] However, the expected growth of the surface plasmon resonance band (SPR) of Au nanoparticles at about 550 nm was not observed with respect to a decrease of the $AuCl_4^-$ anion absorption band.

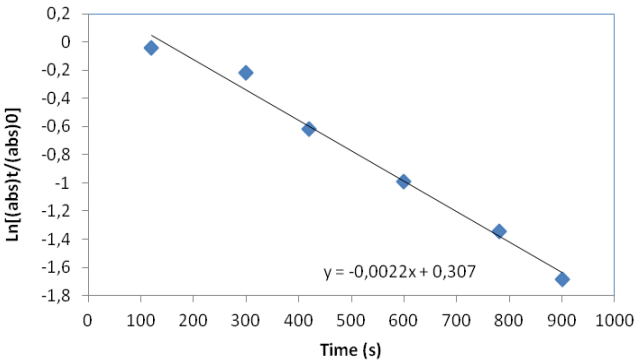

Figure 2. Absorbance data at 311 nm from Fig. 1 plotted according to the pseudofirst order kinetics law showing that the reduction of $AuCl_4^-$ anion occurred with a rate constant of $2.2x10^{-3}$ s^{-1}.

Therefore, it should be concluded that in the selected reaction conditions the reduction of Au(III) was stopped at Au(I) stage which was stabilized toward the disproportionation reaction $3Au^+ \rightarrow Au^{3+} + 2Au°$.[42]

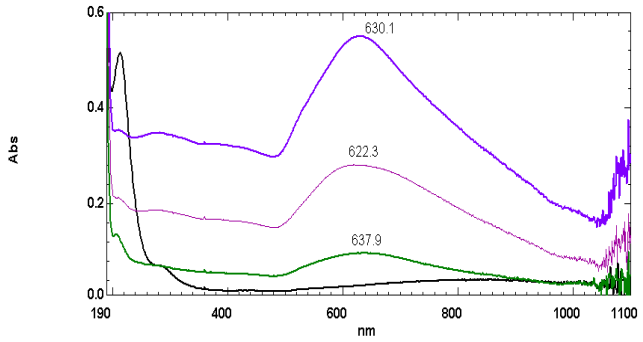

Figure 3. Electronic absorption spectra of gold nanorods. First curve from bottom (black) was taken 2 min after the addition of hydroxylamine to $AuCl_3$; The second curve from bottom (green) is due to the SPR band of colloidal gold taken 5 min after the addition of hydroxylamine. The other two absorption bands (red and violet) on the top were recorded after further additions of $AuCl_3$ in portions of 6 mg each.

At higher dilutions the just mentioned disproportionation reaction becomes feasible and indeed the formation of blue colloidal gold nanoparticles was observed using $AuCl_3•3H_2O$ solutions at a concentration of 1.2 mg/100 ml. Fig. 3 shows the development of the SPR band of gold nanoparticles initially with an absorption peak at 638 nm which is then shifted to 622 nm and then to 630 nm as consequence of further $AuCl_3•3H_2O$ additions to the solution. The formation of colloidal Au nanoparticles acts as seeds for further colloidal gold formation. This is the meaning of Fig. 3, where each increase in the optical density of the SPR band corresponds to a further addition of $AuCl_3•3H_2O$ which is reduced in its turn. The SPR absorption bands of blue gold nanoparticles shown in Fig.3 between 622 and 638 nm appears considerably broad and suggests that gold nanorods with aspect ratio around 2 to 4 were obtained.[43,44] In fact, the absorption spectra of gold nanorods is characterized by the dominant SP_l band (at longer wavelength) corresponding to longitudinal resonance (the peak at 622-630 nm) and a much weaker transverse resonance at shorter wavelength, (about 520 nm) which appears as a broad shoulder in the spectrum of Fig.3.[43,44] An additional contribution to the intensity of the SP_1 band is possible by the amount of Au nanospheres which may exist in the dispersions of gold nanorods.[43]

Ozone effect on gold nanorods

When ozone is bubbled in spherical gold nanoparticles hydrosol, the reduction of the intensity of the SPR band is accompanied by a red shift of the band.[45-47] The entity of the SPR red shift is of the order of 50 nm toward longer wavelengths for a spherical gold hydrosol with average particles diameter of 7 nm and is reduced to only 10 nm red shift toward longer wavelengths when the gold nanoparticles have an average diameter of 32 nm.[47] The explanation of this phenomenon which changes also the color of the colloidal solution is based on the chemisorptions of ozone on the surface of gold nanoparticles. The chemisorptions shifts the electron density of the metal particle toward the adsorbate and consequently there is a change in the Fermi level in each particle.[47]

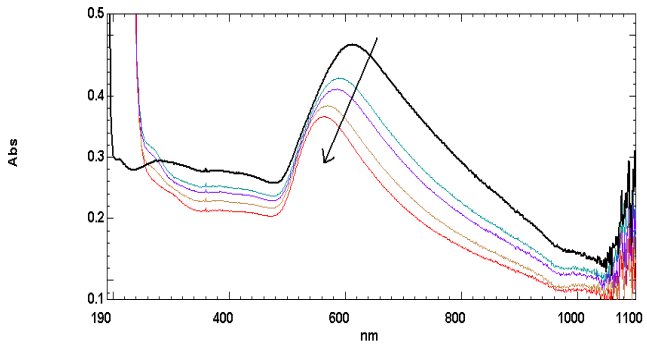

Figure 4. When ozone is bubbled in the colloidal gold nanorods hydrosol the SPR band undergoes a blue shift as indicated by the arrow.

In Fig. 4 is shown for the first time the response of gold nanorods with aspect ratio in the range between 2 and 4 and average diameter between 10 and 15 nm. The trend upon the O_3 adsorption on gold nanorods is exactly opposite to that of spherical nanoparticles reported in literature.[45-47] This time the SPR band experiences a blue shift, or hypsochromic shift: a shift toward shorter wavelengths, rather than the common and known red shift. Furthermore, the entity of the blue shift from 612 nm to a limiting value of 564 nm, i.e. $\Delta\lambda$ = -48 nm is of the same magnitude but opposite sign as that measured on spherical nanoparticles, i.e. $\Delta\lambda \approx 50$ nm.[47] The blue shift effect can be appreciated in Fig. 5, where it is evident that a rapid blue shift $\Delta\lambda$ = -27 nm from 612 nm to 585 nm, it follows a relatively slow further blue shift toward the limiting value of 564 nm with a $\Delta\lambda$ = -48 nm. Curiously, the same trend is observed in Fig. 6 in what is known as hypochromic effect. The absorption intensity of the SPR band falls down with the ozonization time and the shape of the curve of Fig 6 is same as that of the blue shift reported in Fig.5. Thus, not only the SPR band is shifted toward shorter wavelengths but its absorption intensity is also reduced.

Based on these experimental data it looks like that the ozone adsorption on gold nanorods affects almost exclusively the dominant SP_l band (the component at longer wavelength)

corresponding to longitudinal resonance. The suppression of longitudinal resonance provides evidence in Fig. 4 that the residual transverse resonance which occurs at shorter wavelengths and seems much less affected by the ozone adsorption on gold nanorods.

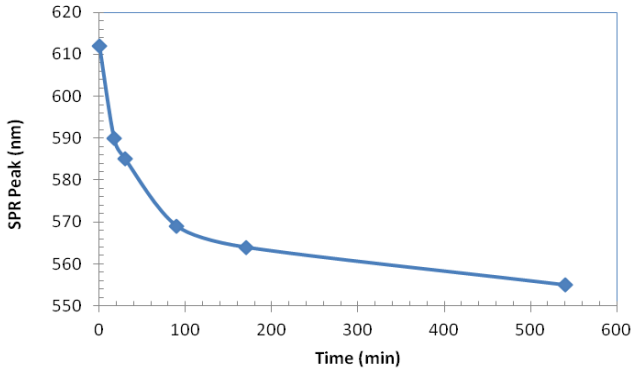

Figure 5. Blue shift of the SPR band when ozone is bubbled in the colloidal gold hydrosol made of nanorods; data from Fig. 4.

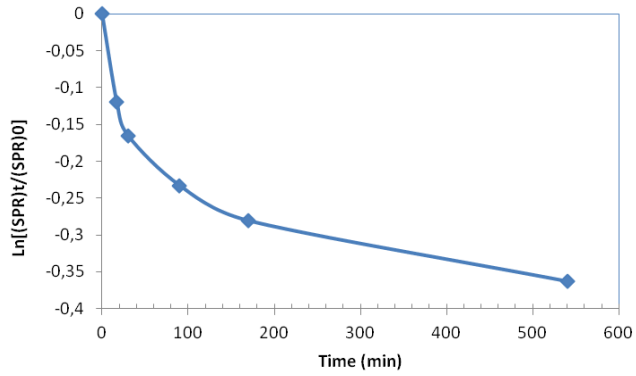

Figure 6. Trend of the SPR band when ozone is bubbled in the colloidal gold nanorod hydrosol; absorbance data from Fig. 4 reported in ordinate as $Ln[(SPR)_t/(SPR)_0]$.

Reduction of $AuCl_3•3H_2O$ with black tea infusion

Black and green tea infusions were successfully used as green reducing and capping agents in silver nanoparticles formation.[2] Black tea infusion was also proposed as a green reducing agent of Au^{3+} with the formation of stable colloidal gold hydrosol.[48] The mechanism of action of tea infusions in the formation of noble metal colloidal nanoparticles is discussed elsewhere.[2] The polyphenols present in the tea infusions are the active agents which cause the reduction of silver or gold ions to metal nanoparticles. Furthermore, the mixture of natural products in tea infusion (see reference 2 for a detailed composition) act as excellent capping agents of the metal nanoparticles stabilizing indefinitely the hydrosol. As described in the experimental section, the production of a nice and stable red gold hydrosol was easily achieved by adding $AuCl_3•3H_2O$ to a diluted black tea infusion. Fig. 7 shows that the initial absorption of the pristine diluted black tea has no absorption features from 400 to 800 nm (the green absorption curve at the bottom of Fig. 7) and the development of the SPR band at 532 nm as a consequence of the addition of $AuCl_3$ to the diluted black tea infusion.

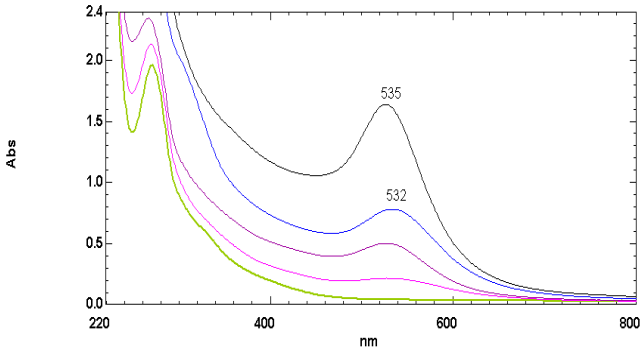

Figure 7. The bottom most green curve is related to prisinte black tea absorption; other curves from bottom to top (red, amaranth, blue and black) are the SPR band of gold nanoparticles formed in diluted black tea infusion.

Each absorption curve was taken after the addition of 5-6 mg of $AuCl_3•3H_2O$, so the final amount of gold was around 22 mg L^{-1}. The blue curve (fourth from the bottom) in Fig. 7 is the curve obtained after the third addition of $AuCl_3•3H_2O$. The absorption curve of the solution left overnight is at the top of Fig. 7 the SPR absorption maximum at 535 nm, slightly shifted to longer wavelengths with respect to the original position at 532 nm. The SPR band in Fig. 7 is narrow and symmetric, completely different than the SPR band discussed in Fig. 3 for gold nanorods. From the SPR peak position, half width of the band and other related considerations,[49] it is possible to conclude that the colloidal particles produced in diluted tea infusion are spherical with an average diameter of 20 nm.

Ozone effect on spherical gold nanoparticles

Fig. 8 shows the spectral evolution of a gold hydrosol when exposed to a continuous stream of ozone. This time the gold hydrosol is constituted by spherical nanoparticles prepared by the action of black tea infusion on $AuCl_3$, as discussed in the preceding section. From Fig. 8 it is evident that the action of ozone on the Au nanoparticles is causing a shift of the SPR toward longer wavelengths (red or bathochromic shift). This phenomenon is already reported in literature,[45-47] and consequently it is confirmed by our experimental results. However, the red shift of the SPR band, is completely in contrast with the results of the preceding experiment discussed in the previous section, when gold nanorods were exposed to ozone showing instead a blue shift in the SPR band position. Since the main difference between the two experiments is the shape of the gold nanoparticles, it can be anticipated here that the shift of the SPR band is deeply affected by the shape of gold nanoparticles.

In Fig. 9 it is reported the entity of the of the red shift of the SPR band in the case of the spherical gold nanoparticles. At the beginning of the ozonization the shift is from 525 nm to 527 nm and to 529 nm involving a $\Delta\lambda = 4$ nm. However, above 90 min of ozone bubbling the SPR band is found at 546 nm with a $\Delta\lambda = 21$ nm. Afterwards the hydrosol was left for 45 min saturated with ozone but without any further O_3 bubbling. As shown in Fig. 8 and reported in Fig. 9, the final SPR peak position was found at 587 nm which corresponds to a red shift $\Delta\lambda = 62$ nm.

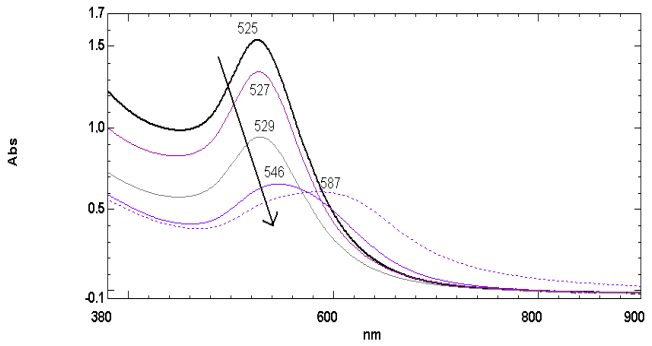

Figure 8. When ozone is bubbled in spherical gold nanoparticles hydrosol there is a red shift of the SPR band as indicated by the arrow.

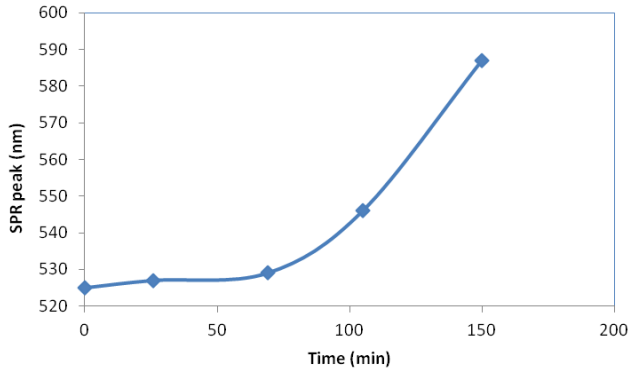

Figure 9. Red shift of the SPR band when ozone is bubbled in the colloidal gold hydrosol of spherical nanoparticles; data from Fig. 8.

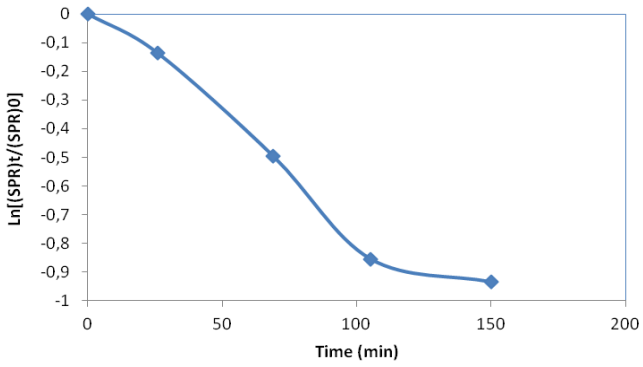

Figure 10. Trend of the SPR band when ozone is bubbled in the colloidal gold hydrosol made of spherical nanoparticles; absorbance data from Fig. 8 reported in ordinate as $Ln[(SPR)_t/(SPR)_0]$.

A similar trend was observed by other authors in the ozonation of spherical gold hydrosol stabilized with citrate.[47] In that case the maximum red shift measured was $\Delta\lambda$ = 50 nm.[47] It would be instructive to compare the blue shift of the SPR in gold nanorods in Fig. 5 with the red shift of the SPR band in spherical gold nanoparticles in Fig. 9 during ozone treatment. In the former case the blue shift is quite fast for the first 100 min then reaching slowly to a limiting value. In the latter case the trend is opposite not only because of the red shift but also because the shift is initially slow at the beginning of the ozonization and becomes faster only after 90 min. In view of the potential application of gold nanoparticles as active sensing material, the gold nanorods seem to ensure a faster response and a higher sensitivity than the spherical gold nanoparticles.

Fig. 10 shows the decreasing absorption intensity of the SPR band as a function of the ozonation time. This hypochromic effect on ozone-treated gold nanoparticles is observed in Fig. 6 and reported in literature.[47] It can be concluded from the comparison of Fig. 6 with Fig. 10 that in the former case the reduction of the intensity SPR is very fast from the beginning of ozonation and then it slows down, following the same trend of the blue shift. The analysis of the curve in Fig. 6 permits to distinguish two stages as suggested by the two slopes which can be derived from the curve. The first step is suggested by a steep slope. In the case of Fig. 10, the reduction of the intensity of the SPR band practically conforms to the pseudo-first order kinetics law up to 100 min of ozonation and afterwards a kind of "saturation" is reached. It must be remembered here that in Fig. 10 the ozonation was interrupted at 105 min. Thus, the latest step to 150 min was achieved in a quiescent state of the hydrosol saturated with ozone.

Discussion

The practical application of the surface plasmon resonance (SPR) transition of metal nanoparticles is more than a promise in analytical and bioanalytical chemistry.[50-54] Indeed, a number of applications are already under development or are being developed under various stages.[49-53] The interaction of gold nanoparticles hydrosol with small molecules was very clearly explained by Ershov and colleagues,[47] and in greater detail by Girault and collaborators.[55] In brief, the chemisorptions of a given molecule, for example ozone, on the spherical gold nanoparticle shifts the electron density of the metal nanoparticle toward the adsorbate. This is accompanied by a reduction in the Fermi level of the gold nanoparticle and the colour of the gold hydrosol changes upon the chemisorption of a given molecule.[47] The change of colour can be measured spectrophotometrically as a shift in the SPR band peak. In particular the interaction of spherical gold nanoparticles hydrosol produces a red shift of the SPR band, a shift toward longer wavelengths or a bathochromic shift.[47] In other words, the SPR transition is less energetic after the chemisorption of a molecule. Ershov and colleagues,[47] have pointed out that the entity of the bathocromic shift is linked to the electron affinity of the analyte being maximum with molecules with high electron affinity (E_A) like O_3, NO_2, Cl_2 respectively with E_A = 2.1-2.4 eV and less pronounced with molecules having lower E_A like SO_2, O_2 (in the range of 1.1 to 0.5 eV). Furthermore, the entity of the bathocromic shift is linked also with the average diameter of the nanoparticles being maximum for smaller nanoparticles ($d \leq 10$ nm).[47,55] A similar way to describe the interaction between ozone and gold surface is to compare their respective ionization potentials which are 12.53 eV for the former and 9.226 eV for the latter.[55] Consequently, it appears obvious that the electrical charge will be displaced from gold surface to the ozone adsorbate. From the entity of the bathocromic or red shift in Fig. 8 and 9 we have measured a $\Delta\lambda$ = 62 nm (which refers to the gold nanoparticle electrons displaced toward the adsorbed ozone), a value significantly larger than $\Delta\lambda$ = 51 nm found by other authors.[50] From the bathochromic

shift $\Delta\lambda$ = 62 nm it is possible to estimate the bonding energy between ozone and gold nanoparticle surface which is 5.75 kcal mol^{-1} or 24.07 kJ mol^{-1}. These values suggest more a charge-transfer complex interaction between adsorbent and adsorbate rather than a real chemisorption.[56]

To explain the blue shift or hypsochromic shift observed in the interaction between gold nanorods and ozone as shown in Fig. 4 and 5 it is necessary to admit that in this case electron charges are injected by the adsorbate to the metal surface. This fact will be accompanied by an increase of the Fermi level in the gold nanoparticles and the entity of the SPR blue shift $\Delta\lambda$ = -48 nm is quite large as in the case of the red shift discussed previously. Also in this case the energy of the SPR displacement can be calculated to ≈ 4 kcal mol^{-1} or 16.63 kJ mol^{-1} in line with the charge-transfer interaction. The blue shift of the SPR band in gold nanorods was detected with electrochemical measurements on a ITO substrate and in other conditions.[57,58]

The reason of this opposite behavior between spherical gold nanoparticles which give a red shift in the SPR band when they interact with ozone and gold nanorods which instead give a blue shift in the interaction with ozone is explainable by the form of the outer nanoparticle potential which in the case of spherical nanoparticle is described by the following equation:[55]

$$\psi_{\text{spherical}} = \frac{Ze}{4\pi\varepsilon r} \quad (1)$$

while for a cylindrical nanoparticle the potential has opposite sign as follows:[59]

$$\psi_{\text{cylinder}} = -\frac{Ze}{2\pi\varepsilon}\ln\frac{r}{R} \quad (2)$$

Since the ionization energy of the nanoparticle is given by:[55]

$$I_{\text{E(NP)}} - I_{\text{Ef}} = e\psi \quad (3)$$

and hence

$$I_{\text{Ef}} = I_{\text{E(NP)}} - \frac{Ze^2}{4\pi\varepsilon r} \quad (4)$$

$$I_{\text{Ef}} = I_{\text{E(NP)}} + \frac{Ze^2}{2\pi\varepsilon r}\ln\frac{r}{R} \quad (5)$$

Equation 4 shows that the energy of the Fermi level of the spherical gold nanoparticle is that of the ionization energy of the nanoparticle lowered by the outer potential given by Eqn. 1. This is the case of the red shift of the SPR band and charges donated from the nanoparticle to the adsorbate. Equation 5 instead illustrates the opposite case, that relative to gold nanorods , where the energy of the Fermi level is due to the ionization energy of the nanorods enhanced by the outer potential given by Eqn. 2. This is the case of the blue shift of the SPR band and charges injected from the adsorbate to the nanoparticle.

Conclusions

Gold nanoparticles interact with ozone giving a large shift in the SPR band. Spherical gold nanoparticles give a red or bathochromic shift of the SPR band in their interaction with O_3 and the electric charges are donated from the adsorbent spherical nanoparticles to the adsorbate ozone molecules lowering the Fermi level of the metal nanoparticles. Gold nanorods interact with ozone more readily than gold nanospheres. Gold nanorods give a blue or hypsochromic shift of the SPR band in their interaction with O_3 and the electric charges are injected by the adsorbate ozone molecule to the adsorbent gold nanorods. The opposite behavior of gold nanospheres and gold nanorods toward ozone can be explained by the different sign and equation form of the potential developed respectively by the two geometrical structures.

References

[1]Cataldo, F., Ursini, O., Angelini, G., *Eur. Chem. Bull. Sect. B.,* **2013**, *2*, 700.

[2]Cataldo, F., *Eur. Chem. Bull. Sect. B.,* **2014**, *3*, 280.

[3]Cataldo, F., Ursini, O., Angelini, G., *J. Radioanal. Nucl. Chem.*, **2016**, published online, DOI 10.1007/s10967-015-4141-2.

[4]Sharma, V.K., Yngard, R.A., Lin, Y., *Adv. Colloid Interface Sci.* **2009**, *145*, 83.

[5]Abou El-Nour, K. M.. M., Eftaiha ,A., Al-Warthan, A., Ammar, R. A. A., *Arabian J. Chem.,* **2010**, *3*, 135.

[6]Tolaymat, T. M., El Badawy, A. M., Genaidy, A., Scheckel, K. G., Luxton, T. P., Suidan, M., *Sci. Total Environ.,* **2010**, *408*, 999.

[7]Moritz, M., Geszke-Moritz, M., *Chem. Eng. J.,* **2013**, *228*, 596.

[8]Mittal, A. K., Chisti, Y., Banerjee, U. C., *Biotechnol. Adv.* **2013**, *31*, 346.

[9]Sharma, T. K., Chopra, A., Sapra, M., Kumawat, D., Patil, S. D., Pathania, R., Navani, N. K., *Int. J. Green Nanotech.*, **2012**, *4*, 1.

[10]Roy, N., Gaur, A., Jain, A., Bhattacharya, S., Rani, V., *Environ. Toxicol. Pharmacol.*, **2013**, *36*, 807.

[11]Kharissova, O. V., Dias, H. V. R., Kharisov, B. I., Olvera Perez, B., Perez, V. M. J., *Trends Biotechnol.*, **2012**, *31*, 240.

[12]Cataldo, F., *Fullerenes, Nanotubes Carbon Nanostruct.,* **2014**, *23*, 523.

[13]Cataldo, F., Iglesias-Groth, S., *Fullerenes, Nanotubes Carbon Nanostruct.,* **2014**, *23*, 253.

[14]Cataldo, F., Hafez,Y., Iglesias-Groth, S., *Fullerenes, Nanotubes Carbon Nanostruct.,* **2015**, *23*, 1037.

[15]Cataldo, F., Putz, M. V., Ursini, O., Hafez, Y., Iglesias-Groth, S., *Fullerenes, Nanotubes Carbon Nanostruct.,* **2015**, *23*, 1095.

[16]Hayat, M. A. (Ed.) "*Colloidal Gold: Principles, Methods and Applications*" Vol. 1, Academic Press, San Diego, **1989**, Chapter 2.

[17]Daniel, M. C., Astruc, D. , *Chem. Rev.*, **2004**, *104*, 293.

[18]Mingos, D. M. P. (Ed.) "*Gold Clusters, Colloids and Nanoparticles*", Structure and Bonding Series Vol. 161, Springer, Heidelberg, **2014**.

[19]Wikipedia,:"*ColloidalGold*"https://en.wikipedia.org/wiki/Colloidal_gold#cite_note-Sharma.2C_RK_2012-36 .

[20]Henglein, A., Meisel, D., *Langmuir*, **1998**, *14*, 7392.

[21]Jana, N. R., Gearheart, L., Murphy, C. J., *Adv. Mater.*, **2001**, *13*, 1389.

[22]Sun, Y., Xia, Y., *Science*, **2002**, *298*, 2176.

[23]Eustis, S., El-Sayed, M. A., *Chem. Soc. Rev.*, **2006**, *35*, 209.

[24]Grzelczak, M., Pérez-Juste, J., Mulvaney, P., Liz-Marzán, L. M., *Chem. Soc. Rev.*, **2008**. *37*, 1783.

[25]Ho, V. A., Le, P. T., Nguyen, T. P., Nguyen, C. K., Nguyen, V. T., Tran, N. Q., *J. Nanomater.*, **2015**, *2015*, Article ID 241614, 7 pages.

[26]Nisha, M. H., Tamileaswari Sr, R., Jesurani, S., *Int.. J. Eng. Sci. Res. Technol.*, **2015**, ***4***, 733.

[27]Tufail, A., *J. Nanotech.*, **2014**, *2014*, Article ID 954206, 11 pages.

[28]Cruz,, S. M. A., Nogueira, H. I. S., Marques, P. A. A. P., *Ciência Tecnol. Mater.*, **2014**, *26*, 102.

[29]Chekuri, M., Gangarudraiah, S., Roopavatharam, L. B., Kaphle, A., Chalimeswamy, A. *Eur. Chem. Bull.*, **2015**, *4*, 454.

[30]Praba, P. S., Vasantha, V. S., Jeyasundari, J., Jacob, Y. B., *Eur. Chem. Bull.*, **2015**, *4*, 117.

[31]Pavliashvili, T., Kalabegishvili, T., Janjalia, M., Ginturi, E., Tsertsvadze, G., *Eur. Chem. Bull.*, **2015**, *4*, 30.

[32]Brown, C. L., Bushell, G., Whitehouse, M. W., Agrawal, D. S., Tupe, S. G., Paknikar, K. M., Tiekink, E. R., *Gold Bull.*, **2007**, *40*, 245.

[33]Brown, C. L., Whitehouse, M. W., Tiekink, E. R. T., Bushell, G. R.. *Inflammopharmacology*, **2008**, *16*, 133.

[34]Wikipedia, "*Gold Nanoparticles in Chemotherapy*", https://en.wikipedia.org/wiki/Gold_nanoparticles_in_chemotherapy .

[35]Giljohann, D. A., Seferos, D. S., Daniel, W. L., Massich, M. D., Patel, P. C., Mirkin, C. A., *Angew. Chem. Int. Ed.*, **2010**, *49*, 3280.

[36]Galdiero, S., Falanga, A., Vitiello, M., Cantisani, M., Marra, V., Galdiero, M., *Molecules*, **2011**, *16*, 8894.

[37]Muñoz, A., Sigwalt, D., Illescas, B. M., Luczkowiak, J., Rodríguez-Pérez, L., Nierengarten, I., Holler, M., Remy, J. S., Buffet, K., Vincent, S. P., *Nature Chem.*, **2016,** *8*, 50.

[38]Dwivedi, A. D., Dubey, S. P., Sillanpää, M., Kwon, Y. N., Lee, C., Varma, R: S., *Coord. Chem. Rev.* **2015**, *287*, 64.

[39]Ghosh, S. K., Pal, T., *Chem. Rev.*, **2007**, *107*, 4797.

[40]White, R. G., "*Handbook of Ultraviolet Methods*", Plenum Press, New York, **1965**, methods 1516 and 1518.

[41]Soni, V., Mehrotra, R. N., Mechanism of the oxidation of hydrazoic acid by tetrachloroaurate (III) ion. *Transition Metal Chem.*, **2008**, *33*, 367-376.

[42]Housecroft, C. E., Sharpe, A. G., "*Inorganic Chemistry*" 3rd Ed., Pearson Education, Harlow, Essex, UK,**2008**, p. 795.

[43]Yu, Y. Y., Chang, S. S., Lee, C. L., Wang, C. R. C., *J. Phys. Chem. B*, **1997**, *101*, 6661.

[44]Sharma, V., Park, K., Srinivasarao, M., *Matei. Sci. Eng.*, **2009**, *65*, 1.

[45]Puckett, S. D., Heuser, J. A., Keith, J. D., Spendel, W. U., Pacey, G. E. *Talanta*, **2005**, *66*, 1242

[46]Pisarenko, A. N., Spendel, W. U., Taylor, R. T., Brown, J. D., Cox, J. A., Pacey, G. E., *Talanta*, **2009**, *80*, 777.

[47]Ershov, B. G., Abkhalimov, E. V., Roldughin, V. I., Rudoy, V. M., Dement'eva, O. V., Solovov, R. D., *Phys. Chem. Chem. Phys.*, **2015**, *17*, 18431.

[48]Sharma, R. K., Shikha G., Shilpa M., *J. Chem. Educ.*, **2012**, *89*, 1316.

[49]Haiss, W., Thanh, N. T., Aveyard, J., Fernig, D. G., *Anal. Chem.*, **2007**, *79*, 4215.

[50]Aoki, P. H., Constantino, C. J., Oliveira Jr, O. N., Aroca, R. F.. "Plasmonics in Analytical Spectroscopy" Chapter 14 in *ACS Symposium Series*, **2015**, *1215*, 43.

[51]Maier, S. A. "*Plasmonics: fundamentals and applications.*" Springer, Heidelberg, **2007**.

[52]Uechi, I., Yamada, S., *Anal. Bioanal. Chem.*, **2008**, *391*, 2411.

[53]Chon, J. W. M., Iniewsk, K. (Ed.), "*Nanoplasmonics: Advanced Device Applications*", CRC Press, Taylor & Francis Group, Boca Raton, **2014**.

[54]Valcarcel, M., Lopez-Lorente, A. I., "*Gold Nanoparticles in Analytical Chemistry*", Elsevier, Amsterdam, **2014**.

[55]Scanlon, M. D., Peljo, P., Méndez, M. A., Smirnov, E., Girault, H. H., *Chem. Sci.*, **2015**, *6*, 2705.

[56]Gregg, S. J., "*The Surface Chemistry of Solids*", Chapman & Hall Ltd, London, **1965**, p.84-95.

[57]Novo, C., Funston, A. M., Gooding, A. K., Mulvaney, P., *J. Am. Chem. Soc.*, **2009**, *131*, 14664.

[58]Chen, H., Shao, L., Li, Q., Wang, J., *Chem. Soc. Rev.*, **2013**, *42*, 2679.

[59]Benenson, W., Harris, J. W., Stocker, H., Lutz, H. (Ed.) "Handbook of Physics", Springer-Verlag, New York, **2002**, p.450.

.

Received: 14.01.2016.
Accepted: 19.02.2016.